APPLICATION OF CONSTRAINED GIBBS ENERGY MINIMIZATION TO NUCLEAR FUEL THERMOCHEMISTRY

H. LOUKUSA, V. VALTAVIRTA
Nuclear Safety, VTT Technical Research Centre of Finland
P.O. Box 1000, FI-02044 VTT - Finland

ABSTRACT

The modelling of the chemical composition of nuclear fuel is a complex problem due to the numerous fission products formed during fuel operation and their possibility to form various chemical compounds. The application of Gibbs energy minimization to model the chemical composition requires the assumption that the fuel is at local thermochemical equilibrium when the fuel is thermally in a steady state. The temperature through the pellet radius can vary 1000 K, with highest temperatures found in the pellet center. Depending on the local fuel temperature, the validity of the local equilibrium approximation varies, as diffusion and chemical kinetics limit the formation of the thermodynamically most stable species. At the fuel surface, the state of the fuel is farthest from equilibrium.

However, with constrained Gibbs energy minimization it is possible to investigate the thermochemically most favourable state of the fuel in cases where the composition of the fuel is not at equilibrium. As a first application on nuclear fuel, the effect of cesium iodide vaporization and radiolysis in a radiation field is investigated with constrained Gibbs energy minimization. A kinetic model for cesium iodide radiolysis is used to determine a steady state, which is then used to constrain the equilibrium calculated for a nuclear fuel pellet surface. The feedback from such an analysis can be used to further refine kinetic models, as the thermochemical equilibrium calculation yields information on the possibly important species that a kinetic model should consider.

1 Introduction

Nuclear fuel is a very complex mixture of actinides and fission products where an exceedingly large number of different chemical compounds can form. For such a complex mixture, Gibbs energy minimization provides a powerful tool for the prediction of its chemical composition in the thermochemical (local) equilibrium state. However, it is this last requirement - essential for the use of the method - that complicates such analyses.

The assumption of local thermochemical equilibrium assumes that for a local region of space, all components of the system are ideally mixed throughout the system, every reaction has proceeded to equilibrium and there is a constant temperature and pressure. Typical uranium oxide-based nuclear fuel is a solid material, where diffusion of some elements is slow, so the system is not ideally mixed. Less information is available on the kinetics of the reactions between fission products, but it should be safe to say that many reactions do not reach their equilibrium before some other parameter of the system changes. High temperature conditions accelerate diffusion and reaction kinetics. Even though nuclear fuel is typically operated at a relatively high temperature, where different parts of the fuel pellet experience temperatures from 500 to 1500 K in normal operation, this is not enough for a solid material to be completely mixed by diffusion, or that the rate of all reactions are very fast.

Thermochemical investigations of nuclear fuel are possible even with these limitations, and several studies have been published in recent years [1, 2, 3, 4]. Very useful qualitative and sometimes even quantitative information can be obtained from such studies. However, the

methods can be refined to obtain more accurate quantitative information or new qualitative information that cannot be obtained with traditional thermochemical modelling. One such method is the calculation of non-equilibrium states with constrained Gibbs energy minimization. As a first application to nuclear fuel, the radiolysis of cesium iodide was selected as it effectively involves a single chemical reaction, the dissociation or vaporization of cesium iodide. The dissociation of cesium iodide in a radiation field is important as cesium iodide is unreactive towards nuclear fuel cladding, whereas atomic and molecular iodine are ~~not~~reactive. Reactive iodine species can cause stress corrosion cracking of the cladding [5], so the formation of such species is unfavorable towards cladding integrity.

2 Theoretical background

2.1 Constrained Gibbs energy minimization

Gibbs energy minimization involves the calculation of mole amounts of species whose combination yields the minimum of Gibbs energy at constant temperature and pressure. The quantity to be minimized is the total Gibbs energy of the system, which can be calculated as the following sum:

$$G = \sum_{i}^{S} \mu_i n_i,$$

where S is the number of species in the system, μ_i the chemical potential and n_i the mole amount of species i. In a traditional Gibbs energy minimization calculation, only material constraints for the total Gibbs energy are used. In general, the material constraints for the mole amounts of species in a minimization calculation are given as

$$\sum_{i}^{S} a_{ij} n_i = b_j,$$

where a_{ij} is the stoichiometric coefficient of constraint j in species i and b_j is the value of constraint i in moles.

However, it is also possible to limit the minimum with other, immaterial constraints. These constraints are not related to the mole amounts of components (often chemical elements) in the system, but other constraining factors, such as chemical reaction kinetics. The method of setting kinetic constraints in the constrained free energy (CFE) method is described in detail by Koukkari [6] and Pajarre [7]. A kinetic constraint is applied in the minimization calculation as an additional constraint and an additional column of the stoichiometric matrix of the system. Koukkari et al. use virtual species to input the values of these constraints. The virtual species allow for conservation of derived thermodynamic quantities in process chemical calculations. It is also possible to directly input the value of the constraint so that no virtual species are needed in the system, which is done in this work. The immaterial constraint effectively dictates the formation or decomposition of the species for which the stoichiometric coefficient of the immaterial constraint is nonzero.

The maximum possible value of the immaterial constraint must also respect the mass balance of the system. In practice, the value of the constraint in a kinetically constrained calculation is determined through an unconstrained equilibrium calculation and the kinetic model. The kinetic model gives us the extent of the reaction, ξ, which can be used to constrain the equilibrium. The extent of reaction is a quantity relating the changes in mole amounts of reactants and products and has the unit of moles. When a reaction $v_A A \leftrightarrow v_B B$

proceeds so that dξ of A reacts, the change in mole amount of A is $dn_A = - v_A d\xi$, and for B, $n_B = v_B d\xi$. At the beginning of a reaction, ξ is defined as 0.

At thermochemical equilibrium, ξ has some value ξ_{eq}, and at a non-equilibrium state some value ξ_{neq}. For the minimization, the value of the immaterial constraint, or the mole amount of the immaterial component, is then set as

$$b = \xi_{neq}.$$

A benefit of a thermodynamic equilibrium calculation is that several thermodynamic variables can be easily calculated from the results. One such quantity is the affinity of a chemical reaction, which is the "driving force" behind a chemical reaction as defined by De Donder [8]. The meaning of the "driving force" can be illustrated through the rate of production of entropy. This rate due to a chemical reaction can be defined as the product of the thermodynamic force, the "driving force", with the corresponding thermodynamic flow [~~8~~9]:

$$\frac{dS}{dT} = \left(\frac{A}{T}\right)\left(\frac{d\xi}{dt}\right),$$

where the first term containing the affinity A is the thermodynamic force and the second term the thermodynamic flow in the chemical reaction defined through the extent of reaction. As can be seen from the above equation, the time dependence of the rate of entropy production is not contained within the affinity, as it is determined by the thermodynamic flow.

The affinity is positive if the reaction happens spontaneously, and can be derived from the constraints' potentials that are calculated during the minimization. Each constraint has a potential Γ_j associated with it, and in a Lagrange multiplier method these are the Lagrange coefficients of the constraints. The constraint potentials are related to the chemical potentials of the species in the system as

$$\mu_i = \sum_j^C a_{ij}\Gamma_j.$$

Additionally, for each imaginable reaction

$$\sum_i \nu_i \mu_i = 0,$$

where species i participate in the reaction. However, for a kinetically constrained reaction the above reaction does not apply as the sum is nonzero, and equal to the negative of the partial derivative of Gibbs free energy with respect to the extent of reaction, or the thermodynamic affinity A [6]:

$$\sum_i \nu_i \mu_i = -\frac{\partial G}{\partial \xi} = -A.$$

The previous equations also imply that at equilibrium, affinity is zero. Affinity can also be defined through the immaterial constraint potential as

$$A = -\sum_i \nu_i \sum_{j=C+1}^{C'} a_{ij}\Gamma_j.$$

where C is the number of material constraints, and C' the number of immaterial constraints.

2.2 Applied kinetic model

Several cesium iodide radiolysis models can be found from the literature. Ball et al. [10~~9~~] and Filin et al. [1~~1~~0] have applied a full radiation-chemical kinetic model to cesium iodide radiolysis. Ball et al. have additionally investigated the radiolysis of cesium telluride. Filin et al. have even taken into account the effect of oxygen-containing species on the kinetics. However, in both cases many of the reaction rate constants have been assumed as typical for a type of reaction, as there is little experimental data available. Konashi et al. [12~~1~~, 13~~2~~] have modelled fewer reactions, but these reaction rates are mostly based on experimental data. In part due to this and the simplicity of the Konashi et al. model it is applied in this work.

Konashi et al. [12~~1~~, 13~~2~~] have considered two types of radiation: fission fragments themselves and the atoms of the collision cascade caused by those fragments. The reaction rates are calculated based on collision theory. The Konashi model includes the species Cs, I, I_2 and CsI, three equilibria and two decomposition reactions. In this work, the decomposition reactions have been combined into a single effective decomposition reaction, and a vaporization-condensation equilibrium has been added.

$$\mathrm{Cs} + \mathrm{I} \underset{k_{r1}}{\overset{k_{d1}}{\leftrightharpoons}} \mathrm{CsI}$$

$$2\mathrm{I} \underset{k_{r2}}{\overset{k_{d2}}{\leftrightharpoons}} \mathrm{I_2}$$

$$\mathrm{Cs} + \mathrm{I_2} \underset{k_{r3}}{\overset{k_{d3}}{\leftrightharpoons}} \mathrm{CsI} + \mathrm{I}$$

$$\mathrm{CsI} \underset{k_{d4}}{\overset{\rightarrow}{}} \mathrm{Cs} + \mathrm{I}$$

$$\mathrm{CsI\ (s)} \underset{k_{v5}}{\overset{k_{c5}}{\leftrightharpoons}} \mathrm{CsI\ (g)}$$

The rate constants were taken from [~~11~~12], but the model was updated with a new energy distribution for the fission fragments at the fuel surface. The model by Konashi et al. assumes a flat energy distribution, but actually due to geometric considerations, the energy distribution is peaked at low energies [~~13~~14] and has the following probability distribution function:

$$\frac{1}{8E_{max}}\left(\frac{E}{E_{max}}\right)^{-\frac{1}{2}},$$

where E_{max} is the kinetic energy of the fission fragment at the time of fission. Low energy fission fragments are also those that most effectively dissociate cesium iodide into its constituent elements. The rate constant k_{d4} is the sum of the rate constants for fission fragment irradiation, k_{ff}, and energetic gas atom induced irradiation, k_{Xe}, which were calculated to be (in s^{-1}):

$$k_{ff} = 2A_{ff}\dot{F}RE_{max}^{-\frac{1}{2}}(-0.991E_{max} + 0.395E_{max}logE_{max} + 1.72), \text{and}$$

$$k_{Xe} = A_{Xe}\dot{F}(0.0919 + 2.71E_{max}^{-2.16} - 1.16E_{max}^{-1.16}).$$

In the above equations, $\dot{F}$ is the fission rate, R is the fission fragment range in the fuel matrix, A_{ff} a constant with the value of $4.467 \cdot 10^{-13}$ cm^2 and A_{Xe} a constant with a value of $2.93 \cdot 10^{-16} \cdot \exp(2.6 \cdot 10^{-3} \cdot T)$ cm^2.

The condensation and vaporization rate constants were estimated in this work. The condensation rate onto the pellet surface was derived from a simple relation by Langmuir derived from the ideal gas law and the kinetic theory of gases, and for a section of the fuel rod it is

$$k_{r5} = -\sqrt{2\pi MRT}rh,$$

where M is the molar mass of cesium iodide, R the gas consant, r the fuel pellet radius and h the height of the section of the fuel rod. The vaporization rate is calculated through the energy deposited by fission fragments as they pass through a cesium iodide layer on fuel grain surfaces. Only the surface exposed to the fuel pellet-cladding gap is allowed to vaporize. The energy deposition rate is calculated as

$$\dot{E}_{dep} = \frac{\dot{F}RE_{max}}{3}\left(1 - \left(1 - \frac{z}{R_{CsI}}\right)^2\right),$$

where z is the thickness of the cesium iodide layer and R_{CsI} is the range of the fission fragments in cesium iodide (estimated as 3.77 µm). The vaporization rate is then obtained by dividing the deposited energy with the energy ΔH required to vaporize solid cesium iodide, which is about 2.2 eV:

$$\frac{dn}{dt} = \frac{\dot{E}_{dep}}{\Delta H}.$$

3 Methodology

The kinetic model was solved with a MATLAB program. The solution to the differential equations is obtained with the *ode23s* solver as the problem is stiff. A previously developed Gibbs energy minimization routine is used in the thermochemical equilibrium calculations [4]. The routine has been extended for easy application of immaterial constraints in the minimization. The mole amounts of the fuel were calculated for a PWR rod with Serpent. The values used in the calculations correspond to those at the surface node at a burnup of approximately 60 MWd·kg$_U^{-1}$. The calculated mole amounts used in the final constrained equilibrium calculation are shown in table 1, where the mole amounts of all elements are combined into "representative elements" as in [4].

Table 1. Mole amounts of fission products relative to the amount of uranium.

Representative element	Amount (mol/mol U)	Representative element	Amount (mol/mol U)
H	$3.00 \cdot 10^{-5}$	I	0.0022
Y	0.0034	Xe	0.0418
Zr	0.0298	Cs	0.0218
Mo	0.0304	Ba	0.0165

Tc	0.0069	La	0.0082
Ru	0.0256	Ce	0.0163
Rh	0.0041	Pr	0.0069
Pd	0.0233	Nd	0.0306
Te	0.0051	Pu	0.0398

Most thermochemical data is obtained from the Royal Military College of Canada Fuel Thermochemical Treatment published in [~~14~~15], except that of gaseous TeI_2, which is taken from [~~15~~16], and the enthalpy of $UMoO_6$ which has been changed according to [~~16~~17, ~~17~~18]. The equilibrium constants used in the calculation of k_{d1} and k_{r2} through the law of mass action were calculated with data from the RMC fuel model. In the constrained calculations, the formation of solid iodine species were suppressed. In the gas phase, the gaseous cesium iodide dimer was excluded from the calculation, as the model in this work does not take into account its radiolysis.

4 Results

The gas phase kinetic model was first verified with initial values similar to the work of Konashi et al. In their work, the initial cesium metal concentration was slightly higher than that of cesium iodide, and iodine species concentrations much lower than those. With such initial values, the steady-state values of the kinetic model were found in the case where there is radiation ($k_{d4} \neq 0$) and where there is not $k_{d4} = 0$). With radiation, the atomic iodine gas concentration rose 10^9-fold, and for molecular iodine gas 10^8-fold. These results are roughly in agreement with the work of Konashi et al.

In the work of Konashi et al., it was assumed that the equilibrium concentrations of iodine species are much lower than those of cesium and cesium iodide. Their values were based on a simple thermochemical analysis. However, a detailed thermochemical equilibrium calculation on fuel reveals that the equilibrium concentrations of atomic and molecular iodine may be much higher.~~,~~ As can be seen in figure 1, they may be~~and~~ only an order of magnitude smaller than that of cesium iodide at high temperatures and, at low temperatures, even higher than that of cesium iodide~~, as can be seen in figure 1~~. Furthermore, the concentration of cesium iodide in the gas phase drops with increasing oxygen content in the fuel, as cesium is oxidized, whereas the concentration of iodine species increases. The effect of radiolysis in this case would be negligible.

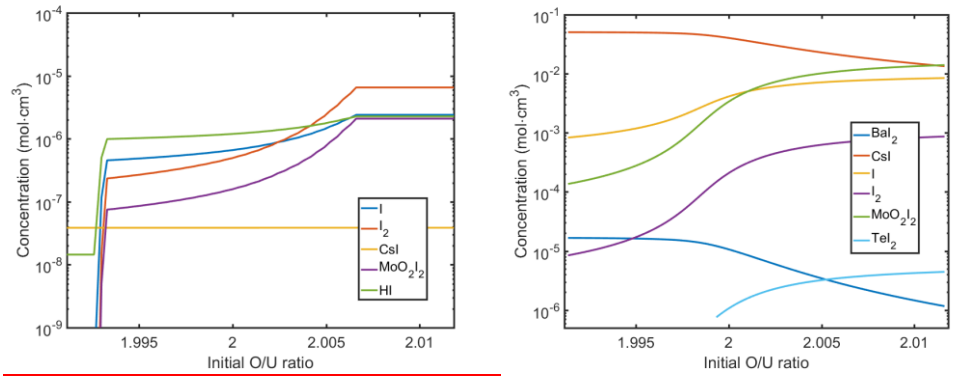

Figure 1. Concentrations of the most abundant gas phase species containing iodine at a temperature of ~~1473 K (right) and~~ 773 K (left) and 1473 K (right).

The case where cesium iodide radiolysis would have a larger effect is at such a temperature where cesium iodide is a solid or a liquid. The temperature in the fuel-cladding gap is typically such that cesium iodide appears as a solid. This case can be modelled by augmenting the gas phase model with a cesium iodide vaporization-condensation reaction as described in section 3.

Solving the kinetic model with radiation we find that the condensation and vaporization reactions reach a steady state very quickly, in less than a second. In the steady state, most solid cesium iodide that is exposed to the gap is vaporized. The radiolysis of gaseous cesium iodide does not appear to have much of an effect on the gas phase concentrations of atomic and molecular iodine. This is presumably because the concentrations are initially already quite high compared to those calculated by Konashi et al. [~~8~~12], for example, and their ratio is closer to unity.

The mole amount of solid cesium iodide corresponding to the extent of reaction ξ_{neq} can be calculated from these results and used as an immaterial constraint in the Gibbs energy minimization. This way the thermodynamically most stable species that would form from the cesium and iodine freed by radiolysis can be determined.

First, we shall see how the affinity of the cesium iodide vaporization reaction changes as a function of the extent of reaction. This is done by changing the extent of reaction input as an immaterial constraint incrementally from the equilibrium value. The change in affinity is shown in figure 2, with the vertical line showing the extent of reaction determined from the results of the kinetic model. The change in affinity has a peculiar feature around a ξ of $1.0 \cdot 10^{-5}$, where the magnitude of the affinity starts to ~~increase~~ decrease suddenly. The sign of affinity is defined by the direction of the reaction: for the condensation reaction, the affinity would increase. –The concentrations of gaseous cesium and hydrogen iodides in figure 2 show why this happens. The limiting value for hydrogen iodide corresponds to the amount of hydrogen in the system; therefore no additional hydrogen iodide can form. The excess vaporized iodine from this point on forms gaseous cesium iodide.

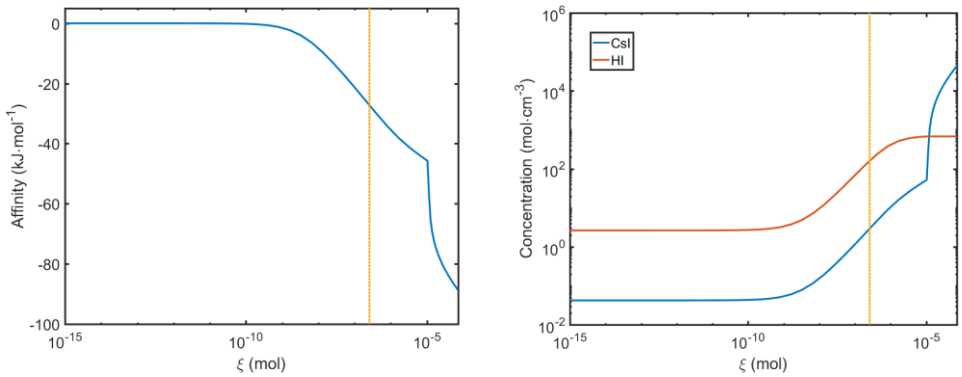

Figure 2. The thermodynamic affinity of the cesium iodide vaporization reaction and the mole amounts of cesium and hydrogen iodides as functions of the extent of reaction of the vaporization reaction.

The concentrations of the main iodine-containing species at equilibrium and at constrained equilibrium are shown in table 1, along with the values calculated by just the kinetic model. Interestingly, it is not gaseous cesium iodide that increases most in its mole amount, but hydrogen iodide. The reaction of hydrogen with iodine to form hydrogen iodide appears to be very favourable thermodynamically at this temperature, more favourable than cesium iodide.

Hydrogen in this calculation is derived purely from nuclear reactions occurring in nuclear ~~fule~~ fuel during irradiation. Unfortunately it is currently not possible to obtain information from Serpent on which reactions contribute to the amount of each element. Probable reactions producing hydrogen isotopes include ternary fission and $^{16}O(n,p)^{16}N$.~~.~~

Formatted: Superscript

Formatted: Superscript

Table 1. Concentrations of the main iodine containing species at equilibrium, the steady-state from the kinetic model and the constrained equilibrium.

	Concentration ($mol \cdot cm^{-3}$)			
Species	Kinetic	Equilibrium	Constrained equilibrium	Iodine fraction
BaI_2		$8.95 \cdot 10^{-10}$	$4.29 \cdot 10^{-6}$	0.048
CsI	$1.78 \cdot 10^{-4}$	$4.07 \cdot 10^{-8}$	$2.82 \cdot 10^{-6}$	0.016
HI		$2.54 \cdot 10^{-6}$	$1.55 \cdot 10^{-4}$	0.855
I	$4.36 \cdot 10^{-10}$	$2.90 \cdot 10^{-8}$	$2.01 \cdot 10^{-6}$	0.011
I_2	$1.52 \cdot 10^{-8}$	$9.84 \cdot 10^{-10}$	$4.72 \cdot 10^{-6}$	0.053
MoO_2I_2		$3.15 \cdot 10^{-10}$	$1.51 \cdot 10^{-6}$	0.017
TeI_2		$2.37 \cdot 10^{-12}$	$1.14 \cdot 10^{-8}$	$1.28 \cdot 10^{-4}$

Formatted: Space After: 3 pt

Formatted: Space After: 3 pt

Formatted: Space After: 3 pt

5 Summary

Hydrogen iodide seems to be a more thermodynamically favourable form of iodine than cesium iodide at low temperatures. Its reaction with zirconium is also favourable, as can be seen from figure 3, where the Gibbs energies of reaction for various reactive iodine species with zirconium metal are shown. The iodine is thought to form gaseous zirconium tetraiodide, ZrI_4, with the zirconium metal. It can therefore be possible that also hydrogen iodide plays a role in iodine stress corrosion cracking.

The formation of hydrogen iodide requires hydrogen, which is formed in small amounts through nuclear reactions. It can also be present as an impurity, such as residual moisture from the fuel pellet manufacturing process. Hydrogen present also as an impurity would increase the amount of hydrogen iodide calculated to form in this work.

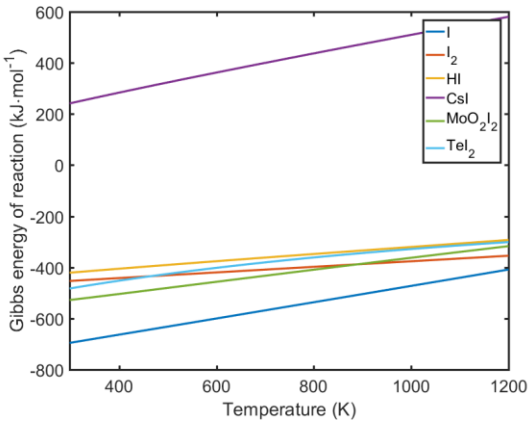

Figure 3. Gibbs energies of reaction with zirconium to zirconium tetraiodide for the most abundant iodine species.

6 Acknoledgements

This work was funded by personal grants from the Fortum Foundation. The author would like to thank Pertti Koukkari and Risto Pajarre at VTT for their help on the constrained free energy method and Timo Ikonen on his help on the early phases of this work.

7 References

[1] Piro, M. H. A., Banfield, J., Clarno, K. T., Simunovic, S., Besmann, T. M., Lewis, B. J., & Thompson, W. T. (2013). Coupled thermochemical, isotopic evolution and heat transfer simulations in highly irradiated UO2 nuclear fuel. Journal of Nuclear Materials, 441(1–3), 240–251.

[2] Baurens, B., Sercombe, J., Riglet-Martial, C., Desgranges, L., Trotignon, L., & Maugis, P. (2014). 3D thermo-chemical-mechanical simulation of power ramps with ALCYONE fuel code. Journal of Nuclear Materials, 452(1–3), 578–594.

[3] Besmann, T. M., McMurray, J. W., & Simunovic, S. (2016). Application of thermochemical modeling to assessment/evaluation of nuclear fuel behavior. Calphad: Computer Coupling of Phase Diagrams and Thermochemistry, 55, 47–51.

[4] Loukusa, H., Ikonen, T., Valtavirta, V., & Tulkki, V. (2016). Thermochemical modeling of nuclear fuel and the effects of oxygen potential buffers. Journal of Nuclear Materials, 481, 101–110.

[5] Cox, B. (1990). Pellet-clad interaction (PCI) failures of zirconium alloy fuel cladding - A review. Journal of Nuclear Materials, 172(3), 249–292.

[6] Koukkari, P. (2014). Introduction to constrained Gibbs energy methods in process and materials. Espoo, Finland: VTT Technical Research Centre of Finland. Retrieved from http://www.vtt.fi/inf/pdf/technology/2014/T160.pdf.

[7] Pajarre, R. (2016). Modelling of chemical processes and materials by free energy minimisation. PhD thesis. Aalto University.

[8] De Donder, T. and Van Rysselberghe, P. Thermodynamic theory of affinity - A book of principles. Stanford University Press, Stanford, CA, USA, 1936. 142 p.

[9] Kondepudi, D. and Prigogine, I. Modern thermodynamics - From heat engines to dissipative structures. John Wiley & Sons, Chichester, UK, 1998. 506 p.

Formatted: Centered

[10] R. G. J. Ball,W. G. Burns, J. Henshaw, M. A. Mignanelli, P. E. Potter (1989). The chemical constitution of the fuel-clad gap in oxide fuel pins for nuclear reactors, Journal of Nuclear Materials, 167, 191–204.

[11] V. M. Filin, V. V. Novikov, A. S. Sotnikov, S. M. Bogatyr', V. I. Kuznetsov, (2014). Particulars of the effect of the internal medium of a fuel element in high-burnup fuel on the corrosion cracking of fuel-element cladding under stress, Atomic Energy, 115, 1–6.

[12] Konashi, K., Yato, T., & Kaneko, H. (1983). Radiation effect on partial pressure of fission product iodine. J. Nucl. Mater., 116, 86–93.

[13] Konashi, K., Yamawaki, M., & Yoneoka, T. (1988). CsI decomposition due to collision cascade initiated by fission fragments. Journal of Nuclear Materials, 160, 75–80.

[14] van Reenen, T. J. and de Wet, W, J. (1970). Equations for the computer computation of the kinetic energy distributions of fission fragments released from nuclear fuel surfaces by recoil. Technical report PEL-198, Pelindaba, South Africa.

[15] Thompson, W. T., Lewis, B. J., Piro, M. H., Corcoran, E. C., Kaye, M. H., Higgs, J. D., … Thompson, D. M. (2012). RMC Fuel Thermochemical Treatment, Department of Chemistry and Chemical Engineering, Royal Military College of Canada, Kingston, ON, Canada.

[16] Kut'in, a. M., Polyakov, V. S., Churbanov, M. F., & Snopatin, G. E. (2007). Vapor pressure and thermodynamic functions of TeI4 and its decomposition products. Inorg. Mater., 43(9), 1018–1023.

[17] Corcoran, E. C., Kaye, M. H., & Piro, M. H. A. (2016). An overview of thermochemical modelling of CANDU fuel and applications to the nuclear industry. Calphad: Computer Coupling of Phase Diagrams and Thermochemistry, 55, 52–62.

[18] Dash, S., Jayanthi, K., Singh, Z., Dahale, N. D., Parida, S. C., & Iyer, V. S. (2000). Calorimetric studies on uranium molybdate. Journal of Alloys and Compounds, 296, 166–169.~~[8] Kondepudi, D. and Prigogine, I. Modern thermodynamics - From heat engines to dissipative structures. John Wiley & Sons, Chichester, UK, 1998. 506 p.~~

~~[9] R. G. J. Ball,W. G. Burns, J. Henshaw, M. A. Mignanelli, P. E. Potter (1989). The chemical constitution of the fuel-clad gap in oxide fuel pins for nuclear reactors, Journal of Nuclear Materials, 167, 191–204.~~

~~[10] V. M. Filin, V. V. Novikov, A. S. Sotnikov, S. M. Bogatyr', V. I. Kuznetsov, (2014). Particulars of the effect of the internal medium of a fuel element in high-burnup fuel on the corrosion cracking of fuel-element cladding under stress, Atomic Energy, 115, 1–6.~~

~~[11] Konashi, K., Yato, T., & Kaneko, H. (1983).~~ Radiation effect on partial pressure of fission product iodine. J. Nucl. Mater., 116, 86–93.

~~[12] Konashi, K., Yamawaki, M., & Yoneoka, T. (1988).~~ CsI decomposition due to collision cascade initiated by fission fragments. Journal of Nuclear Materials, 160, 75–80.

~~[13] van Reenen, T. J. and de Wet, W, J. (1970). Equations for the computer computation of the kinetic energy distributions of fission fragments released from nuclear fuel surfaces by recoil. Technical report PEL-198, Pelindaba, South Africa.~~

~~[14] Thompson, W. T., Lewis, B. J., Piro, M. H., Corcoran, E. C., Kaye, M. H., Higgs, J. D., … Thompson, D. M. (2012). RMC Fuel Thermochemical Treatment, Department of Chemistry and Chemical Engineering, Royal Military College of Canada, Kingston, ON, Canada.~~

~~[15] Kut'in, a. M., Polyakov, V. S., Churbanov, M. F., & Snopatin, G. E. (2007). Vapor pressure and thermodynamic functions of TeI4 and its decomposition products. Inorg. Mater., 43(9), 1018–1023.~~

~~[16] Corcoran, E. C., Kaye, M. H., & Piro, M. H. A. (2016). An overview of thermochemical modelling of CANDU fuel and applications to the nuclear industry. Calphad: Computer Coupling of Phase Diagrams and Thermochemistry, 55, 52–62.~~

~~[17] Dash, S., Jayanthi, K., Singh, Z., Dahale, N. D., Parida, S. C., & Iyer, V. S. (2000). Calorimetric studies on uranium molybdate. Journal of Alloys and Compounds, 296, 166–169.~~

Formatted: English (U.S.)

Formatted: Font: Not Bold

Formatted: Heading 1

Formatted: Outline numbered + Level: 1 + Numbering Style: 1, 2, 3, … + Start at: 1 + Alignment: Left + Aligned at: 0 cm + Indent at: 1 cm

Formatted: English (U.S.)

Formatted: English (U.S.)

Formatted: Heading 1

Formatted: Outline numbered + Level: 1 + Numbering Style: 1, 2, 3, … + Start at: 1 + Alignment: Left + Aligned at: 0 cm + Indent at: 1 cm

Formatted: Heading 1